

1 **Detection of simulated leaks from geologically stored CO₂ with ¹³C monitoring**

2

3 Christophe Moni* and Daniel P. Rasse

4

5 *Bioforsk – Norwegian Institute for Agricultural and Environmental Research. Frederick A.*

6 *Dahls vei 20, Aas, Norway.*

7

8 *Corresponding author (christophe.moni@bioforsk.no)

9 Phone number: +4792020175

10

11 Abbreviations: CCS, carbon capture and storage; CRDS, cavity ring down spectrometer

12

13 **Abstract**

14

15 Precise methods for the detection of geologically-stored CO₂ within and above soil surfaces are
16 an important component of the development of carbon capture and storage (CCS) under
17 terrestrial environments. Although CO₂ leaks are not expected in well-chosen and operated
18 storage sites, monitoring is required by legislation and any leakage needs to be quantified under
19 the EU Emissions Trading Directive. The objective of the present research was to test if ¹³C
20 stable isotope monitoring of soil and canopy atmosphere CO₂ increases our detection sensitivity
21 for CCS-CO₂ as compared with concentration monitoring only. A CO₂ injection experiment
22 was designed to create a horizontal CO₂ gradient across 6×3-m plots, which were sown with
23 oats in 2011 and 2012. Injected CO₂ was methane derived and had an isotopic signature of -
24 46.2‰. The CO₂ concentrations were measured within the soil profile with passive samplers
25 and at several heights within the crop canopies. The CO₂ fluxes and their ¹³C signatures were
26 also measured across the experimental plots. In situ monitoring and gas samples measurements
27 were conducted with a cavity ring down spectrometer (CRDS). The plots displayed hot spots
28 of injected-CO₂ leakage clearly detectable by either concentration or isotopic signature
29 measurements. In addition, the ¹³C signature measurements allow us to detect injected CO₂ in
30 plot regions where its presence could not be unequivocally ascertained based on concentration
31 measurement alone.

32

33 **Keywords:** CO₂ geological storage, leakage monitoring, stable isotopes

34

35

36 1. Introduction

37

38 Precise methods for the detection of geologically-stored CO₂ within and above soil surfaces are
39 an important component of the development of carbon capture and storage (CCS) under
40 terrestrial environments (Winthagen et al., 2005). Although CO₂ leaks are not expected in well
41 chosen and operated storage sites, monitoring is required by legislation and any leakage needs
42 to be quantified under the EU Emissions Trading Directive. Most methods for potential leak
43 detection are geared either towards 1) the rapid detection of the leaking CO₂ itself, 2) changes
44 in soil properties and gas composition or 3) the accumulated impact on plant communities. The
45 latter set of methods has seen multiple applications of airborne and ground-based hyper- and
46 multi-spectral imaging of reflectance plant spectra (Bateson et al., 2008; Chen et al., 2012;
47 Hogan et al., 2012; Jiang et al., 2012; Keith et al., 2009; Lakkaraju et al., 2010; Male et al.,
48 2010; Noomen et al., 2008, 2012; Pickles and cover, 2004; Rouse et al., 2010; Smith et al.,
49 2004; Zhou et al., 2012). Direct biological monitoring based on plant survey also been used
50 (Noble et al., 2012; Opperman et al., 2010). Other soil methods include soil resistivity
51 measurements (Strazisar et al., 2009; Zhou et al., 2012), as well as tracers such as,
52 perfluorocarbon, noble gas, radiocarbon and stable isotope (Bachelor et al., 2008; Fessenden et
53 al., 2010; Garcia et al., 2012; Krevor et al., 2010; McAlexander et al., 2011; Magnier et al.,
54 2012; Pekney et al., 2012; Strazisar et al., 2009; Watson and Sullivan et al., 2012; Wells et al.,
55 2010). Direct CO₂ monitoring methods tested in recent years include eddy covariance mapping
56 of soil fluxes (Lewicky and Hilley 2009; Lewicky et al., 2012), laser based methods for CO₂
57 concentration detection (Barr et al., 2011; Humphries et al., 2008), atmospheric gas
58 concentration ratios analysis (Fessenden et al., 2010; Keeling et al., 2011) and soil gas
59 concentration ratios analysis (Beaubien et al., 2013 ; Romanak et al., 2012).The stable isotope
60 signature of CO₂, i.e. $\delta^{13}\text{C}$, is a method that apportions C sources from multiple source
61 components. For natural sources, this method has been used to quantify the heterotrophic vs.
62 autotrophic components of soil respiration (Biasi et al., 2012; Braig and Tupek, 2010). For
63 fossil fuel sources, this method has been successfully used since the early 1980's to quantify
64 accumulated fossil-fuel CO₂ in the atmosphere (Keeling et al., 1979). Recent studies suggest
65 that $\delta^{13}\text{C}$ monitoring can be used to detect a geological contribution from soil CO₂ efflux
66 (Krevor et al., 2010; McAlexander et al., 2011; Spangler et al., 2010). The source of
67 accumulated CO₂ uptake by plants can also be traced through the $\delta^{13}\text{C}$ signature of plant tissue,

68 such as shown for a polluted urban area (Lichtfouse et al., 2003). In theory, the isotopic method
69 increases our detection limit as compared to concentration measurements alone, and thereby is
70 especially useful at low concentration and low flux rate values. Although a leak taking place
71 through the soil might have a localized CO₂ hotspot, low concentrations are expected over a
72 larger affected area as well as in the atmosphere and in the exposed plants. For monitoring
73 purposes, detecting these low contributions from geologically-stored CO₂ might be critical. The
74 objective of the present study was to quantify geologically-stored CO₂ contributions with the
75 ¹³C isotopic method across a field-simulated horizontal gradient and along the soil-plant-
76 atmosphere continuum.

77
78

79 **2. Materials and Methods**

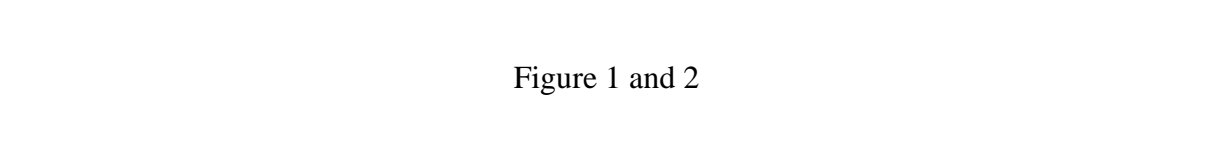
80

81 2.1. Experimental approach

82

83 A subsurface simulated leakage experiment was designed to create a CO₂ gradient within the
84 soil and in the near-surface atmosphere to test different levels of exposure in a cropped field.
85 The gradient was created by injecting CO₂ in a permeable sand layer buried under a less
86 permeable topsoil layer (Fig. 1).

87

88 

89

90 2.2. Experimental site and design of the research plots

91

92 An agricultural silt loam soil (USDA classification) developed on a moraine deposit was
93 selected for the simulated CO₂ injection. The experimental site, designed to assess the impact
94 of a CO₂ leakage on field crops, was located 30 km south east of Oslo (59°36'50" N; 11°00'08"
95 E) (Fig. 2). Two plots, each 6×3 m, were excavated down to 85 cm depth. "T" shaped injection
96 pipes were installed at the bottom of the sand layer at one end of the plot. Pits were first refilled
97 with a 45 cm thick layer of sand (hydraulic conductivity 95 ± 19 m day⁻¹), and then with 40 cm
98 of local topsoil (hydraulic conductivity 11 ± 13 m day⁻¹) so that plot surfaces were level with
99 the surrounding soil. No impervious barrier was used between sand and subsoil (hydraulic
100 conductivity 0.03 ± 0.04 m day⁻¹). For the continuous supply of CO₂, the research plots were
101 connected via buried pipes to a gas delivery system which consisted of a semi-automatic gas

102 panel designed for uninterrupted gas supply. The gas panel was connected to two bundles of 12
103 bottles of 50 l CO₂ each. Switch-over between the two connected bundles occurred when the
104 pressure of one side (the primary side) fell below a pre-set pressure level. This was achieved
105 by two integrated regulators which were connected at their outlet ports. The CO₂ selected for
106 injection was produced from natural gas combustion and exhibited a $\delta^{13}\text{C}$ signature of -46.2 ‰,
107 which is more negative than either atmospheric CO₂ ($\delta^{13}\text{C} \approx -8 \text{ ‰}$) or biogenic CO₂ ($\delta^{13}\text{C} \approx -$
108 26 ‰) at the site.

109
110

111 2.3. Experimental plot management

112

113 In May 2012 experimental plots were disc-ploughed and sown with oats (*Avena sativa*) at the
114 same time as the agricultural field in which they are located. Plots were equipped along the
115 central transect with soil CO₂ probes within one week of ploughing and before emergence of
116 the plants. CO₂ injection started in the second half of June in both plots at a rate of 2 l min⁻¹ and
117 was stopped at the end of the growing season in late August. For plot 1, gassing was interrupted
118 between 29-06-2012 and 11-07-2012 because the gas supply pipe broke. Control values were
119 obtained from side measurements performed in the adjacent oats culture.

120
121

122 2.4. Continuous monitoring of meteorological parameters

123

124 An automatic weather station (Seba Hydrometrie) was installed at the experimental site. The
125 station was equipped with two ultrasonic wind sensors installed at 1 m and 6 m to measure wind
126 speed and direction at canopy height and above the canopy, respectively. The station also has a
127 combined air humidity/temperature sensor located at 20 cm depth, a pressure sensor, a soil
128 temperature sensor, an automated rain gauge, and a global radiation sensor. Data were recorded
129 every 15 min.

130
131

132 2.5. Gas measurements systems

133

134 CO₂ concentration and isotopic signature analyses were performed with a wavelength scanned
135 Cavity Ring Down Spectrometer (WS-CRDS) manufactured by Picarro (Crosson et al., 2008).

136 The instrument was recalibrated to ensure accurate isotopic measurement for a wide range of
137 CO₂ concentration and the processing software was upgraded to reduce transient concentration
138 response and water vapor interference. Methane interferences were accounted for through direct
139 laser measurements of ¹²CH₄ and built-in automatic post corrections. All upgrades and tunings
140 were performed following manufacturer instructions which should ensure precisions of < 0.1
141 ppm and 0.25 ppm in CO₂ stable or transient conditions, respectively. For more security, water
142 vapor interference was further accounted for by pre-drying the sampled gas to <1000 ppm_v
143 water with a Nafion filter. The instrument was field installed in a trailer located 10 m from the
144 experimental plots. The gas sampling rate was 24 ml min⁻¹ and measurements were conducted
145 every 2.7 ± 1.2 second. Sampling was conducted at multiple locations in the canopy with a
146 single 20-m long Teflon tube connected to the instrument. The sampling tube was moved manually
147 to different sampling points.

148 For **continuous atmospheric CO₂ sampling in plot 1**, the gas inlet was placed 5 cm above
149 ground at a distance of 50 cm from the plot border on the gas-injection side. Continuous
150 sampling took place in July for selected periods that did not overlap the mapping periods.

151 **Soil CO₂** was sampled at 20 cm depth from six silicone probes (Kammann et al., 2001)
152 positioned at 50, 150, 250, 350, 450 and 550 cm from the injection side of the plot along the
153 central transect of each plot. Compared to other soil CO₂ sampling methods, the silicone probe
154 methods present the advantage of not creating mass flow in the soil matrix from undefined
155 location (Kammann et al., 2001). CO₂ samples were collected one month after the beginning of
156 the gassing with a 60 ml syringe and diluted in a flow of CO₂-free air to bring the concentration
157 within the detection range of the CRDS. This was performed to monitor the underground
158 migration of the injected gas. Preliminary results from 2011 showed that equilibrium of soil
159 CO₂ concentration is reached within two weeks for an injection rate of 1 l min⁻¹. Control values
160 for soil CO₂ concentration at 20-cm depth were derived from the 2011 experiment.

161 **Atmospheric CO₂** was sampled using a device designed for simultaneous sampling at 12
162 different points within the canopy. Briefly, each sampling line was connected to a gas bag. Each
163 gas bag was itself hermetically enclosed within an individual plastic box. All plastic boxes were
164 connected together to a vacuum pump. At sampling, simultaneous evacuation of the 12 boxes
165 resulted in a simultaneous inflation of the 12 enclosed gas bags. The content of each gas bag
166 was then directly analysed on the CRDS. Atmospheric sampling was carried out 1 month after
167 the beginning of the injection when the plants were 70 cm tall, at the surface of plot 1 following
168 a 50 x 50 cm grid sampling pattern and in the canopy atmosphere at 10, 20, 30 cm from the
169 ground along three longitudinal transects, each of them including seven sampling points.

170 Control values were obtained from the adjacent oats field presenting similar characteristics to
171 that of the experimental plots.

172 **Soil CO₂ fluxes and their isotopic signatures** were mapped after oats harvest on a 60 x 60 cm
173 grid sampling pattern using dark static chambers (60 x 60 x 20 cm) directly connected to the
174 CRDS by a Teflon line. Static chambers were deployed for 7 minutes. Soil CO₂ fluxes were
175 directly derived from the recorded CO₂ accumulation in the chambers, whereas the isotopic
176 signature of CO₂ was derived from changes in both CO₂ content and isotopic ratio by graphical
177 resolution of the resulting Keeling plot (Keeling, 1958). Control values were estimated from
178 measurements performed on a zone adjacent to the experimental plot with similar topsoil
179 properties.

180

181

182 2.6. Vegetation sampling

183

184 At the end of the growing season (August/September), each plot was harvested on a 50 x 50 cm
185 grid and each bundle was then dried at 60 °C for 3 days. To determine whether the injected
186 labelled CO₂ had been assimilated by the biomass ten leaves were randomly collected from
187 each bundle, ground to 200 µm using a ball mill and then analysed for their C content and δ¹³C
188 signature with a CRDS coupled to a combustion module (Picarro- CM-CRDS).

189

190 2.7. Data treatment

191

192 To reduce the large number of data generated by the continuous CO₂ monitoring, the original
193 data set was subsampled at a regular 3 min interval. Interpolated maps were obtained by using
194 a default variogram (slope =1, nuggets effect = 0) with Surfer 11.2.848 ©1993-2012, Golden
195 Software, Inc... For interpolation purposes, values measured over a given surface, such as soil
196 CO₂ flux and plant isotopic signature, were attributed to the center of the sampling surface. All
197 other figures were made with SigmaPlot 11.0 ©2008 Systat Software, Inc.

198

199 3. Results

200

201 3.1. Soil CO₂ analysis at 20 cm depth

202

203 In plot 1, soil CO₂ concentrations ranged between 34%, just above the injection point, and 14%
204 at 450 cm from the gassed side of the plot (Fig. 3). Although the highest concentration was
205 found above the injection point, concentration did not show a steady decrease with increasing
206 distance from the gassed side of the plot. Isotopic signature steadily increased from -47‰ to -
207 43‰ with increasing distance from the gassed side of the plot (Fig. 3).

208 In the half of plot 2 nearest to the injection point, CO₂ concentrations ranged between 36% and
209 55% with a maximum at 150 cm from the gassed side whereas in the second half of the plot
210 CO₂ concentration averaged $2.2 \pm 0.3\%$ (Fig. 3). Similarly the soil $\delta^{13}\text{C}$ signature averaged -
211 $44.3 \pm 0.8 \text{ ‰}$ in the gassed half of the plot and $-24.5 \pm 0.3 \text{ ‰}$ in the second half of the plot (Fig.
212 3).

213 Control non-gassed topsoil averaged for the whole growing season a CO₂ concentration of ~3%
214 and isotopic signature of -25‰. Comparing these control values to that of gassed plots indicates
215 that injected CO₂ at 20 cm depth had travelled all along the length of plot 1 and only in the first
216 half of plot 2. Uneven variation of the CO₂ concentrations along the central transect might
217 indicate changes in soil properties, such as compaction, porosity, cracks, or water content.
218 Isotopic values slightly lower than that of injected CO₂ (i.e. -46.2 ‰) were observed during
219 preliminary tests and could be explained by fractionation processes that can occur in the soil,
220 such as partial dissolution of injected CO₂ or at the CO₂ probe level due to differential CO₂
221 diffusion.

222
223 Figure 3
224

225 3.2. Soil CO₂ fluxes and associated isotopic signature

226 Soil fluxes ranged between 404.3 and 2.3 ml CO₂ m⁻² min⁻¹ in plot 1, between 566.3 and 4.8 ml
227 CO₂ m⁻² min⁻¹ in plot 2 and averaged $3.7 \pm 1.2 \text{ ml CO}_2 \text{ m}^{-2} \text{ min}^{-1}$ in the control plots (Fig. 4).
228 These values are equivalent to flux rates ranging between 1088.8 and 6.3 g CO₂ m⁻² day⁻¹ for
229 plot 1, and between 1525.0 and 13.0 g CO₂ m⁻² day⁻¹ for plot 2, with an average control flux of
230 $9.9 \pm 3.1 \text{ g CO}_2 \text{ m}^{-2} \text{ day}^{-1}$. Flux distribution was spatially uneven with several distinct zones of
231 moderate and high flux, as well as some irregularly-shaped low flux regions. Hotspots were all
232 located in the first half of the plot, mostly along the edges of the plots (Fig. 4) but also above
233 the injection point (Fig. 2). In plot 2, extra measurements were performed outside the
234 experimental plots close to the injection point to better define the flux distribution. Low fluxes
235 were mostly in the non-gassed half of the plots. In plot 1, the low flux region seems to extend

236 diagonally from the upper border of the plot at 2 m from the injection side to the lower left
237 corner of the plot, encompassing most of the upper left corner. Moderate fluxes were observed
238 over the remainder of the plot and over most of the plot border even in the upper left corner.
239 These results show that the border of the plots, delimited by soil cracks, acted as a preferential
240 pathway for CO₂, and suggests that the limits of the plot were not impermeable to CO₂. Uneven
241 distribution of the fluxes indicates that the soil structure and properties have controlled CO₂
242 release to the surface.

243 The δ¹³CO₂ values ranged between -51.0 and -29.9 ‰ in plot 1, between -49.1 and -23.7 ‰ in
244 plot 2, and averaged -30.4 ± 1.7 ‰ in the control (Fig. 4). Isotopic signature lower than that
245 of the source gas (i.e. -46.2‰) were observed only for a few flux hotspots whose value
246 exceeded 200 ml CO₂ m⁻² min⁻¹ while the median value for all measurements was 12 ml CO₂
247 m⁻² min⁻¹. This suggests that Keeling plots were difficult to establish at very high rates.
248 However, at such rates, the isotopic method is actually not needed to ascertain the origin of the
249 CO₂ coming out of the soil. In general, spatial distribution of δ¹³CO₂ was inversely related to
250 that of the CO₂ fluxes. In plot 1 however, low flux regions were characterized by δ¹³C values
251 significantly lower than that of the control (mean:-39.6 ‰ vs. -30.4 ‰). This result suggests
252 that although surface CO₂ fluxes were not increased, injected CO₂ had still moved into the soil.
253 Contrastingly in plot 2, low flux regions in the half of the plot furthest from the injection point
254 were characterized by δ¹³C not significantly different from the control, indicating that injected
255 CO₂ had not reached that part of the plot, neither by advection nor diffusion.

256

257

Figure 4

258

259

260 Concerning the CO₂ balance, the total CO₂ flux measured over the entire surface of plots 1 and
261 2 averaged 1.05 and 0.78 l CO₂ min⁻¹, respectively. These measured CO₂ rates account
262 respectively for 52 and 39 % of the actual CO₂ injection rate, which was 2 l CO₂ min⁻¹. Taking
263 into account the extra measurements performed close to the injection point of plot 2 (see Fig.
264 4), the figure rose to 82 % for this plot. This shows that flux rates below 100% can partially be
265 explained by a loss of injected CO₂ out of the monitored area. Also, the closed chamber system
266 designed for measuring diffusive fluxes can potentially underestimate advective fluxes, such as
267 under injected CO₂ conditions.

268

269 3.3. Canopy CO₂ analysis (plot 1)

270

271 At ground level within the canopy atmosphere, CO₂ concentration and δ¹³CO₂ ranged from 432
272 to 10298 ppm and from -12.6 to -45.6 ‰, respectively (Fig. 5). By comparison, in the control
273 plot, CO₂ concentration and δ¹³CO₂ averaged 448 ± 50 ppm and -12.9 ± 2.6 ‰ respectively.
274 The highly correlated Keeling plot (i.e. R²=0.988) displaying an intercept value close to the
275 δ¹³CO₂ of the injected CO₂ (i.e. -45.9 ‰ vs -46.2 ‰), clearly evidenced the mixing of injected
276 and atmospheric CO₂ at ground level (Fig. 6) and enabled the characterization of different
277 leakage intensity. CO₂ leakage as detected at ground level in the atmosphere mostly mimicked
278 the map of the flux distribution. Zones where leaking CO₂ could not be detected were associated
279 with low flux regions, whereas zones where it could be detected were associated with enhanced
280 flux zones. Interestingly the peak of injected CO₂ leakage (i.e. 10298 ppm and -45.6 ‰) that
281 occurred just above the injection point on the central transect was collocated with the largest
282 flux hotspot whereas other flux hotspots occurring on the border of the plot could not be
283 detected by ground level atmospheric CO₂ concentration measurement. This edge effect can be
284 attributed to increased atmospheric mixing due to a gap in the canopy at the border of the
285 experimental plot to allow lateral access to the plot.

286

287 Figure 5

288

289

290 Along the three longitudinal transects, each of them composed of 3 sampling heights, CO₂
291 concentration decreased while δ¹³CO₂ increased with increasing distance from the gassed side
292 of the plot and with increasing sampling height in the canopy (Fig. 5). The influence of leaking
293 CO₂ was most apparent on the central transect just above the injection point. At 30 cm height
294 in the canopy, concentration and isotopic signature ranged between 365 and 542 ppm and from
295 -8.5 and -20.4 ‰, respectively, indicating that leaking CO₂ was still slightly detectable in the
296 canopy at this height. Detection of the injected CO₂ was reduced for parallel transects on either
297 side of the central one. This effect is probably due to the edge effect, which increased
298 atmosphere mixing.

299

300

Figure 6

301

302 3.4. Continuous monitoring of mixing of atmospheric and surface-soil leaked CO₂ within
303 herbaceous plant canopies

304

305 In absence of gassing, continuous CO₂ measurements at 5 cm from the ground above the
306 injection point on the central transect were strongly controlled by biogenic diurnal cycles (Fig.
307 7). During day time, CO₂ concentration and $\delta^{13}\text{CO}_2$ averaged 370 ppm and -10 ‰, respectively
308 (Fig. 7). At night, CO₂ concentrations increased up to ~700 ppm while $\delta^{13}\text{CO}_2$ became more
309 negative to ~-20‰ (Fig. 7). Plotting CO₂ concentration against wind speed showed that peak
310 CO₂ concentration decreased from 700 ppm in stable low-wind condition to atmospheric
311 concentration for wind speeds equal to 6 m.s⁻¹ (Fig. 8). These results clearly demonstrate that
312 turbulent mixing induced by solar radiation tends to enhance the dilution of soil CO₂ in the
313 canopy atmosphere. Simultaneously, reduced CO₂ assimilation by photosynthesis at night
314 induces the accumulation of soil CO₂ in the canopy atmosphere close to the ground. Since soil
315 CO₂ does not share the same isotopic signature as atmospheric CO₂, diurnal variation of the
316 canopy atmosphere only results from differential mixing between days and nights.

317

318 Figures 7 and 8

319

320 Taking advantage of these diurnal variations in CO₂ resulting from the differential mixing of
321 soil and atmospheric sources it was possible to monitor the variation of soil CO₂ isotopic
322 signature with time before and after the gassing to detect the leakage (Fig. 9). Indeed, the
323 average soil CO₂ isotopic signature dropped from -29.8‰ (i.e. C3 plant signature) before
324 injection to -45.8‰ (i.e. injected gas signature) after injection (Fig. 9).

325

326 Figure 9

327

328 3.5. Effect on plants

329

330 Plant isotopic signatures ranged between -28.9 and -32.3 ‰ with an average of -30.9 ‰ (Fig.
331 10). Although differences were not significant, only 5 out of the 72 positions sampled had an
332 isotopic signature ≤ -32 ‰, they were all aligned on the central transect between 0 and 2 m
333 from the gassed side of the plot, that is to say just above the injection points where CO₂ fluxes
334 and concentration in the near ground atmosphere were maximum. This strongly suggests that
335 plant were slightly labeled by the injected/leaking CO₂ (i.e. -46.2 ‰).

336

337

Figure 10

338

339 4. Discussion

340

341 In this study we simulated a hypothetical leak by injecting CO₂ at a rate of 2 l min⁻¹ at 85 cm
342 depth under an agricultural soil along a 2.5 m long perforated pipe. Although the injection rate
343 selected in the present study was about 10 times lower than that of the simulated leakage
344 experiment carried out at the zero emission research and technology (ZERT) station (Lewicki
345 et al., 2010), surface leakage features were very similar. Considering “hot spots” only, CO₂
346 concentrations in the first 30 cm of the soil were equivalent for both sites, i.e. 34-55 % this
347 study vs. 50 % at ZERT. At ZERT, surface CO₂ fluxes reached ~3100 g.m⁻².day⁻¹ (Lewicki et
348 al., 2010; Strazisar et al., 2009). This value is only 50% higher than our measured fluxes at
349 Grimsrud. Considering that the ZERT facility was designed to simulate a hypothetical leakage
350 from a realistic commercial-scale sequestration project characterized by an annual leaking rate
351 of about 0.001% (Spangler et al., 2010), it can be concluded that our simulated leakage
352 experiment is realistic and representative of a leak of similar amplitude.

353 Our study clearly showed that it was possible to track the three dimensional extent of a realistic
354 simulated leak in the soil-canopy-atmosphere continuum. In the soil, CO₂ leakage was spatially
355 heterogeneous but occurred principally above the injection points. In plot 1, injected CO₂
356 travelled along the entire length of the experimental plot whereas in plot 2 it was not detectable
357 more than half-way through the plot. Plot borders appeared to represent preferential CO₂
358 pathways to the atmosphere. In plot 2, most of the injected CO₂ was leaking from the border or
359 outside the experimental plot, indicating that the edge of the plot was permeable to CO₂. This
360 suggests that preferential flow through soil cracks contributed more to soil CO₂ transport than
361 homogeneous porous-media flow. Monitoring the isotopic signature of CO₂ fluxes enabled us
362 to identify regions of the plots displaying specific CO₂ transfer patterns characterized by either
363 strong or weak advection components. Our results suggest that measuring both the CO₂ flux
364 and its isotopic signature enables identification of 3 topsoil zones: 1) zones where the injected
365 gas does not migrate, 2) zones where the injected CO₂ migrates slowly, presumably dominated
366 by the diffusive component, 3) zones where the injected CO₂ migrates rapidly, where advective
367 transport appears dominant. All of these observations suggested a strong control of the leakage
368 pattern by the soil structural properties, such as cracks, compaction, porosity, water content,

369 and hydraulic conductivity. This finding is consistent with results from CO₂ leakage modeling
370 studies (Oldenburg and Unger, 2003, 2004).

371 Once in the atmosphere, leaking CO₂ was quickly diluted by turbulent mixing. Canopy CO₂
372 concentrations were closer to atmospheric values during daytime than nighttime. In a natural
373 system this effect is well documented and largely due to the absence of CO₂ uptake at night
374 (e.g. Rasse et al. 2002). Here, although photosynthetic uptake during daytime might have
375 reduced somewhat canopy-CO₂ concentrations, our results suggest that most of the diurnal
376 pattern was induced by a difference in turbulent mixing between daytime and night time.

377 Maximum canopy CO₂ concentration decreased sharply with increasing wind speed. During
378 daytime, our results show reduced CO₂ concentration with increasing sampling height in the
379 canopy and with the proximity to the edge of the plots. At 30 cm height leaking CO₂ could
380 barely be detected. Finally the accumulation of labeled CO₂ in the canopy resulted in the slight
381 but non-significant modification of the plant isotopic signature, which suggests that uptake of
382 injected CO₂ by the crop canopy was only minimal.

383 Isotopic tracing of surface soil CO₂ efflux allowed us to identify soil regions with low surface
384 emission of the leaked CO₂. These regions displayed soil CO₂ fluxes in the natural range and
385 thereby could not have been identified based on soil CO₂ flux measurements alone. With an
386 injection depth of 85 cm, these low-flux affected regions were located approximately 2 to 5 m
387 away from the source (Fig. 4). Whether this would scale up for deep injected CO₂ is difficult to
388 assess, but our results suggest the potential for detection away from the source in larger regions.
389 In high flux hot spots, the isotopic CO₂ tracing did not appear to bring much additional
390 information compared to measuring CO₂ flux alone, as the simulated leak induced surface CO₂
391 fluxes clearly outside the bounds of normal soil respiration rates.

392 In our case the delineation of low-leakage regions with isotopic tracing was possible because
393 of the contrasted isotopic signature between our CH₄-based CO₂ source at ~-46.2 ‰ and the
394 natural soil CO₂ at -26 ‰, as measured in our control plot. The ZERT detection study was also
395 based on CH₄-derived CO₂ (Spangler et al., 2010). In addition, the large pilot study of Rouse
396 used CH₄-derived CO₂ (Garcia et al., 2012). Natural gas represents about 20% of industrial CO₂
397 emissions (Table 1). Cement factories are large single source emitters producing CO₂ at about
398 0 ‰ (Table 1). The large contribution from liquid and solid fuel combustion, at $\delta^{13}\text{C}$ values
399 of 36 and 35 ‰ respectively, is however very close to natural values for soils of temperate
400 regions (e.g. Beaubien et al., 2013; Risk et al., 2013). This suggests that, beyond pilot studies,
401 stable isotopic tracing of geological CO₂ would be limited to non-mixed reservoirs from CH₄
402 combustion or cement production. Detecting a leakage from a reservoir with CO₂ produced

403 from liquid and solid fuel combustion may however be amenable to other approaches such as
404 gas ratios, noble gas isotopes, or ^{14}C (e.g. Bachelor et al., 2008; Beaubien et al., 2013 ; Risk et
405 al., 2013; Romanak et al., 2012).

406

407

Table 1

408

409 Isotopic monitoring of the geological CO_2 within the soil profile did not appear to increase
410 detection sensitivity as compared to surface flux monitoring. Here we used silicon probes for
411 sampling soil CO_2 as in Kamman et al. (2001). Our silicon probes were non movable and appear
412 to induce a fractionation bias. A recent study suggests that polypropylene probes would not
413 induce fractionation in soils (Parent et al, *in press*). Also, the static nature of the soil-installed
414 probes can be overcome with the barholing method, which consists of directly inserting thin
415 metal pipes into the ground to sample soil CO_2 at different depths and locations (Smith et al.,
416 2004; Al-Traboulsi et al., 2012).

417 Canopy-air $^{13}\text{CO}_2$ monitoring appears to slightly increase detection sensitivity as compared to
418 CO_2 concentration alone (Fig. 5A vs. 5B). However, our results suggest that the sensitivity of
419 the isotopic detection decreases quickly with increasing height in the canopy. Similarly,
420 improved CO_2 detection was reported with isotopic tracing when the inlet was located at 9 and
421 4 cm above the soil surface, as in Krevor et al. (2010) and McAlexander et al. (2011),
422 respectively. This screening technique appears therefore adapted to inlets located right above
423 the soil surface.

424

425 **5. Conclusion**

426

427 The ^{13}C isotopic method proved to be more sensitive than concentration alone for the detection
428 of injected CO_2 . It allowed us to detect low levels of leaking CO_2 when concentration
429 measurements in the range of the natural variation, and enabled the identification of different
430 zones of CO_2 transfer in the soil. In addition, the method enables to identify the source of the
431 CO_2 and thereby confirm a potential CCS origin. While some have suggested that isotopic
432 tracing is a practical detection technique applicable to CSS (Krevor et al., 2010), others report
433 that complex mixing and fractionation processes within a reservoir may alter the isotopic
434 signature of the injected CO_2 and thereby limit its application (Magnier et al., 2012). Although
435 these potential fractionation processes might limit the implementation of $^{13}\text{CO}_2$ isotopic tracing
436 as an operational monitoring tool, they also call for a better understanding of flux pathways,

437 transfer and exchanges in geological and soil layers. With respect to this research need, our
438 study indicates that isotopic monitoring of soil CO₂ fluxes does increase our detection
439 sensitivity and our capacity to map soil regions affected by a simulated CO₂ leakage.

440 Table 1

441

442 **Acknowledgement**

443

444 The present study was part of the RISCS (Research into impacts & safety in CO₂ storage)
445 project whose objective is to provide fundamental research on environmental impacts,
446 necessary to underpin frameworks for the safe management of CO₂ storage sites. RISCS is
447 funded by the EC 7th Framework Programme and by industry partners ENEL I&I, Statoil,
448 Vattenfall AB, E.ON and RWE. R&D partners are BGS, CERTH, IMARES, OGS, PML,
449 SINTEF, University of Nottingham, Sapienza Università di Roma, Quintessa, CO₂GeoNet,
450 Bioforsk, BGR and ZERO. Four R&D institutes outside Europe participate in RISCS: CO₂CRC
451 from Australia, University of Regina from Canada and Montana State and Stanford Universities
452 from the USA. For more information please go to the website ([www.riscs-CO₂.eu](http://www.riscs-CO2.eu)) or contact
453 the project coordinator David Jones (e-mail: dgj@bgs.ac.uk tel. + 44 (0)115 936 3576). Partial
454 funding for this project was also provided by the Norwegian Research Council (project GHG-
455 NOR, NFR 208424). The authors are grateful to Øistein Johansen, Roald Aasen, Hege
456 Bergheim and Raphael Fauches for logistical and technical supports.

457

458 **References**

459

- 460 Al-Traboulsi, M., Sjøgersten, S., Colls, J., Steven, M., Black, C., 2012. Potential impact of CO₂
461 leakage from carbon capture and storage systems on field bean (*Vicia faba*). *Physiol.*
462 *Plant.* 146, 261-271.
- 463 Bachelor, P.P., McIntyre, J.I., Amonette, J.E., Hayes, J.C., Milbrath, B.D., Saripalli, P., 2008.
464 Potential method for measurement of CO₂ leakage from underground sequestration fields
465 using radioactive tracers. *J. Radioanal. Nucl. Ch.* 277, 85-89.
- 466 Barr, J.L., Humphries, S.D., Nehrir, A.R., Repasky, K.S., Dobeck, L.M., Carlsten, J.L.,
467 Spangler, L.H., 2011. Laser-based carbon dioxide monitoring instrument testing during a
468 30-day controlled underground carbon release field experiment. *Int. J. Greenh. Gas. Con.*
469 5, 138-145.

470 Bateson, L., Vellico, M., Beaubien, S.E., Pearce, J.M., Annunziatellis, A., Ciotoli, G., Coren,
471 F., Lombardi, S., Marsh, S., 2008. The application of remote-sensing techniques to
472 monitor CO₂-storage sites for surface leakage: Method development and testing at Latera
473 (Italy) where naturally produced CO₂ is leaking to the atmosphere. *Int. J. Greenh. Gas.*
474 *Con. 2*, 388-400.

475 Beaubien, S E, Jones, D G, Gal, F, Barkwith, A K A P, Braibant, G, Baubron, J C, Ciotoli, G,
476 Graziani, S, Lister, T R, Lombardi, S, Michel, K, Quattrocchi, F and Strutt, M H. 2013.
477 Monitoring of near-surface gas geochemistry at the Weyburn, Canada, CO₂-EOR site,
478 2001–2011. *Int. J. Greenh. Gas Con. 16*(1), S236-S262.

479 Biasi, C., Pitkamaki, A.S., Tavi, N.M., Koponen, H.T., Martikainen, P.J., 2012. An isotope
480 approach based on C-13 pulse-chase labelling vs. the root trenching method to separate
481 heterotrophic and autotrophic respiration in cultivated peatlands. *Boreal. Environ. Res.*
482 *17*, 184-192.

483 Braig, E., Tupek, B., 2010. Separating soil respiration components with stable isotopes: natural
484 abundance and labelling approaches. *Iforest 3*, 92-94.

485 Chen, Y.H., Jiang, J.B., Steven, M.D., Gong, A.D., Li, Y.F., 2012. Research on the Spectral
486 Feature and Identification of the Surface Vegetation Stressed by Stored CO₂ Underground
487 Leakage. *Spectrosc. Spect. Anal. 32*, 1882-1885.

488 Crosson, E.R., 2008. A cavity ring-down analyzer for measuring atmospheric levels of methane,
489 carbon dioxide, and water vapor. *Appl. Phys. B-Lasers O 92*, 403-408.

490 Fessenden, J.E., Clegg, S.M., Rahn, T.A., Humphries, S.D., Baldrige, W.S., 2010. Novel
491 MVA tools to track CO₂ seepage, tested at the ZERT controlled release site in Bozeman,
492 MT. *Environ. Earth. Sci. 60*, 325-334.

493 Garcia, B., Billiot, J.H., Rouchon, V., Mouronval, G., Lescanne, M., Lachet, V., Aimard, N.,
494 2012. A Geochemical Approach for Monitoring a CO₂ Pilot Site: Rouse, France. A
495 Major gases, CO₂-Carbon Isotopes and Noble Gases Combined Approach. *Oil. Gas. Sci.*
496 *Technol. 67*, 341-353.

497 Hogan, J.A., Shaw, J.A., Lawrence, R.L., Lewicki, J.L., Dobeck, L.M., Spangler, L.H., 2012.
498 Detection of Leaking CO₂ Gas With Vegetation Reflectances Measured By a Low-Cost
499 Multispectral Imager. *Ieee J-Stars 5*, 699-706.

500 Humphries, S.D., Nehrir, A.R., Keith, C.J., Repasky, K.S., Dobeck, L.M., Carlsten, J.L.,
501 Spangler, L.H., 2008. Testing carbon sequestration site monitor instruments using a
502 controlled carbon dioxide release facility. *Appl. Optics 47*, 548-555.

503 Jiang, J.B., Steven, M.D., Chen, Y.H., 2012. Use of Leaf Spectral Ratio Indices to Estimate
504 Leaf Relative Water Content of Beetroot Under CO₂ Leakage Stress. *Sensor Lett.* 10,
505 501-505.

506 Kammann, C., Grunhage, L., Jager, H.J., 2001. A new sampling technique to monitor
507 concentrations of CH₄, N₂O and CO₂ in air at well-defined depths in soils with
508 varied water potential. *Eur. J. Soil Sci.* 52, 297-303.

509 Keeling, C.D., 1958. The concentration and isotopic abundances of atmospheric carbon dioxide
510 in rural areas. *Geochim. and Cosmochim. Acta* 13, 322-334.

511 Keeling, C.D., Mook, W.G., Tans, P.P., 1979. Recent Trends in the C-13-C-12 Ratio of
512 Atmospheric Carbon-Dioxide. *Nature* 277, 121-123.

513 Keeling, R.F., Manning, A.C., Dubey, M.K., 2011. The atmospheric signature of carbon capture
514 and storage. *Philos. T. R. Soc. A* 369, 2113-2132.

515 Keith, C.J., Repasky, K.S., Lawrence, R.L., Jay, S.C., Carlsten, J.L., 2009. Monitoring effects
516 of a controlled subsurface carbon dioxide release on vegetation using a hyperspectral
517 imager. *Int. J. Greenh. Gas Con.* 3, 626-632.

518 Krevor, S., Benson, S., Rella, C., Perrin, J.C., Esposito, A., Crosson, E., 2010. Rapid detection
519 and characterization of surface CO₂ leakage through the real-time measurement of C-13
520 signatures in CO₂ flux from the ground. *Geochim. Cosmochim. Acta* 74, A540-A540.

521 Lakkaraju, V.R., Zhou, X.B., Apple, M.E., Cunningham, A., Dobeck, L.M., Gullickson, K.,
522 Spangler, L.H., 2010. Studying the vegetation response to simulated leakage of
523 sequestered CO₂ using spectral vegetation indices. *Ecol. Inform.* 5, 379-389.

524 Lewicki, J.L., Hilley, G.E., 2009. Eddy covariance mapping and quantification of surface CO₂
525 leakage fluxes. *Geophys. Res. Lett* 7, 137-144

526 Lewicki, J.L., Hilley, G.E., 2012. Eddy covariance network design for mapping and
527 quantification of surface CO₂ leakage fluxes. *Int. J. Greenh. Gas Con.* 7, 137-144.

528 Lewicki, J.L., Hilley, G.E., Dobeck, L., Spangler, L., 2010. Dynamics of CO₂ fluxes and
529 concentrations during a shallow subsurface CO₂ release. *Environ. Earth Sci.* 60, 285-297.

530 Lichtfouse, E., Lichtfouse, M., Jaffrezic, A., 2003. delta C-13 values of grasses as a novel
531 indicator of pollution by fossil-fuel-derived greenhouse gas CO₂ in urban areas. *Environ.*
532 *Sci. Technol.* 37, 87-89.

533 Magnier, C., Rouchon, V., Bandeira, C., Goncalves, R., Miller, D., Dino, R., 2012. Surface and
534 Subsurface Geochemical Monitoring of an EOR-CO₂ Field: Buracica, Brazil. *Oil Gas Sci.*
535 *Technol.* 67, 355-372.

536 Male, E.J., Pickles, W.L., Silver, E.A., Hoffmann, G.D., Lewicki, J., Apple, M., Repasky, K.,
537 Burton, E.A., 2010. Using hyperspectral plant signatures for CO₂ leak detection during
538 the 2008 ZERT CO₂ sequestration field experiment in Bozeman, Montana. *Environ. Earth*
539 *Sci.* 60, 251-261.

540 McAlexander, I., Rau, G.H., Liem, J., Owano, T., Fellers, R., Baer, D., Gupta, M., 2011.
541 Deployment of a Carbon Isotope Ratiometer for the Monitoring of CO₂ Sequestration
542 Leakage. *Anal. Chem.* 83, 6223-6229.

543 Moni, C., Rasse, D.P., 2013. Simulated CO₂ Leakage Experiment in Terrestrial Environment:
544 Monitoring and Detecting the Effect on a Cover Crop Using ¹³C Analysis. *Energy*
545 *Procedia* 37, 3479-3485.

546 Noble, R.R.P., Stalker, L., Wakelin, S.A., Pejcic, B., Leybourne, M.I., Hortle, A.L., Michael,
547 K., 2012. Biological monitoring for carbon capture and storage - A review and potential
548 future developments. *Int. J. Greenh. Gas Con.* 10, 520-535.

549 Noomen, M.F., Smith, K.L., Colls, J.J., Steven, M.D., Skidmore, A.K., Van der Meer, F.D.,
550 2008. Hyperspectral indices for detecting changes in canopy reflectance as a result of
551 underground natural gas leakage. *Int. J. Remote. Sens.* 29, 5987-6008.

552 Noomen, M.F., van der Werff, H.M.A., van der Meer, F.D., 2012. Spectral and spatial
553 indicators of botanical changes caused by long-term hydrocarbon seepage. *Ecol. Inform.*
554 8, 55-64.

555 Oldenburg, C.M., Unger, A.J.A., 2003. On Leakage and Seepage from Geologic Carbon
556 Sequestration Sites: Unsaturated Zone Attenuation. *Vadose Zone J.* 2, 287-296.

557 Oldenburg, C.M., Unger, A.J.A., 2004. Coupled vadose zone and atmospheric surface-layer
558 transport of carbon dioxide from geologic carbon sequestration sites. *Vadose Zone J.* 3,
559 848-857.

560 Oppermann, B.I., Michaelis, W., Blumenberg, M., Frerichs, J., Schulz, H.M., Schippers, A.,
561 Beaubien, S.E., Kruger, M., 2010. Soil microbial community changes as a result of long-
562 term exposure to a natural CO₂ vent. *Geochim. Cosmochim. Acta* 74, 2697-2716.

563 Parent, F., Plain, C., Epron, D., Longdoz, B., In press. A new method for continuously
564 measuring the delta13C of soil CO₂ concentrations at different depths by laser
565 spectrometry. *Eur. J. Soil Sci.*

566 Pekney, N., Wells, A., Diehl, J.R., McNeil, M., Lesko, N., Armstrong, J., Ference, R., 2012.
567 Atmospheric monitoring of a perfluorocarbon tracer at the 2009 ZERT Center
568 experiment. *Atmos .Environ.* 47, 124-132.

569 Pickles, A., Cover, W.A., 2005. Hyperspectral geobotanical remote sensing for CO₂ storage
570 monitoring, in: Thomas, D.C., Benson, S. (Eds.), Carbon dioxide capture for storage in
571 deep geologic formations—results from the CO₂ capture project capture and separation
572 of carbon dioxide from combustion sources. Elsevier, San Diego, pp. 1045–1070

573 Rasse, D.P., Stolaki, S., Peresta, G., Drake, B.G., 2002. Patterns of canopy-air CO₂
574 concentration in a brackish wetland: analysis of a decade of measurements and the
575 simulated effects on the vegetation. *Agric. For. Met.* 114, 59-73.

576 Risk, D, McArthur, G, Nickerson, N, Phillips, C, Hart, C, Egan, J and Lavoie, M. 2013. Bulk
577 and isotopic characterization of biogenic CO₂ sources and variability in the Weyburn
578 injection area. *Int. J. Greenh. Gas Con*, 16(1), S263-S275.

579 Romanak, K.D., Bennett, P.C., Yang, C. and hovorka, S.D., 2012. Process-based approach to
580 CO₂ leakage detection by vadose zone gas monitoring at geologic CO₂ storage sites.
581 *Geophys. Res. Lett.*, 39, L15405.

582 Rouse, J.H., Shaw, J.A., Lawrence, R.L., Lewicki, J.L., Dobeck, L.M., Repasky, K.S.,
583 Spangler, L.H., 2010. Multi-spectral imaging of vegetation for detecting CO₂ leaking
584 from underground. *Environ. Earth Sci.* 60, 313-323.

585 Smith, K.L., Steven, M.D., Colls, J.J., 2004. Use of hyperspectral derivative ratios in the red-
586 edge region to identify plant stress responses to gas leaks. *Remote Sens. Environ.* 92, 207-
587 217.

588 Spangler, L.H., Dobeck, L.M., Repasky, K.S., Nehrir, A.R., Humphries, S.D., Barr, J.L., Keith,
589 C.J., Shaw, J.A., Rouse, J.H., Cunningham, A.B., Benson, S.M., Oldenburg, C.M.,
590 Lewicki, J.L., Wells, A.W., Diehl, J.R., Strazisar, B.R., Fessenden, J.E., Rahn, T.A.,
591 Amonette, J.E., Barr, J.L., Pickles, W.L., Jacobson, J.D., Silver, E.A., Male, E.J., Rauch,
592 H.W., Gullickson, K.S., Trautz, R., Kharaka, Y., Birkholzer, J., Wielopolski, L., 2010. A
593 shallow subsurface controlled release facility in Bozeman, Montana, USA, for testing
594 near surface CO₂ detection techniques and transport models. *Environ. Earth Sci.* 60, 227-
595 239.

596 Strazisar, B.R., Wells, A.W., Diehl, J.R., Hammack, R.W., Veloski, G.A., 2009. Near-surface
597 monitoring for the ZERT shallow CO₂ injection project. *Int. J. Greenh. Gas Con.* 3, 736-
598 744.

599 Tans, P., 1981. ¹³C/¹²C of industrial CO₂, in: Bolin, B. (Ed.), SCOPE16: Carbon cycle
600 modelling. John Wiley and sons, England, pp. 127-129.

601 Watson, T.B., Sullivan, T., 2012. Feasibility of a Perfluorocarbon tracer based network to
602 support Monitoring, Verification, and Accounting of Sequestered CO₂. *Environ. Sci.*
603 *Technol.* 46, 1692-1699.

604 Wells, A., Strazisar, B., Diehl, J.R., Veloski, G., 2010. Atmospheric tracer monitoring and
605 surface plume development at the ZERT pilot test in Bozeman, Montana, USA. *Environ.*
606 *Earth Sci.* 60, 299-305.

607 Winthaege, P., Arts, R., Schroot, B., 2005. Monitoring subsurface CO₂ storage. *Oil Gas Sci.*
608 *Technol.* 60, 573-582.

609 Zhou, X.B., Lakkaraju, V.R., Apple, M., Dobeck, L.M., Gullickson, K., Shaw, J.A.,
610 Cunningham, A.B., Wielopolski, L., Spangler, L.H., 2012. Experimental observation of
611 signature changes in bulk soil electrical conductivity in response to engineered surface
612 CO₂ leakage. *Int. J. Greenh. Gas Con.* 7, 20-29.

613

614

615